Research Article

Green Synthesis and Characterization of Zero Valent Iron Nanoparticles from the Leaf Extract of Psidium Guajava Plant and Their Antibacterial Activity

J. Jeyasundari[1]*, P. Shanmuga Praba[1], Y. Brightson Arul Jacob[2], V. S. Vasantha[3] and V. Shanmugaiah[4]

[1]PG & Research Department of Chemistry, NMSSVN College, Madurai, Tamilnadu, INDIA
[2]PG & Research Department of Chemistry, The American College, Madurai, Tamilnadu, INDIA
[3]School of Chemistry, Department of Natural Products, Madurai Kamaraj University, Madurai, Tamilnadu, INDIA
[4]School of Biological Sciences, Department of Microbial Technology, Madurai Kamaraj University, Madurai, Tamilnadu, INDIA

Abstract

Green synthesis of metallic nanoparticles has accumulated an ultimate interest over the last decade due to their distinctive properties that make them applicable in various fields of science and technology. Metal nanoparticles that are synthesized by using plants have emerged as nontoxic and ecofriendly. In this study, a very cheap and simple conventional heating method was used to obtain the iron nanoparticles (FeNPs) using the extract obtained from the leaves of Psidium guajava *plant*. The obtained iron nanoparticles were characterized by UV-Vis spectroscopy, FTIR spectroscopy, XRD, Cyclic Voltammetry, SEM-EDAX and the antibacterial activity was studied against *Bacillus cereus, Escherichia coli, Klebsiella pneumonia, and Staphylococcus aureus* by the standard disc diffusion method. The synthesized FeNPs were found to be 27nm which was confirmed by XRD.

Keywords: FeNPs, Psidium guajava, UV-Vis, FTIR, XRD, Cyclic Voltammetry, SEM-EDAX

***Correspondence**
Author: J. Jeyasundari
Email: jjsundari16@gmail.com

Introduction

Matter can be broadly divided into two categories based on the size: Macroscopic and Mesoscopic. A Macroscopic matter is visible to the naked eye whereas mesoscopic particles such as bacteria and cells that have dimensions on the order of micron(s), can be observed with optical microscopes. Falling into the gap between the microscopic and the mesoscopic is another class of matter, the nanoscopic particles. [1]. Nanotechnology is a very broad area comprising of nanomaterials, nanotools, and nanodevices [2]. Nanoscale iron particles are recently in great interest in environmental remediation circles in the removal of organic and inorganic pollutants from aqueous solutions [3]. The attention in zero-valent iron nanoparticles has been increasing considerably since the growth of a green production technique in which extracts from leaves are used [4, 5]. Nowadays iron nanoparticles (Fe NPs) are synthesized by plant extracts and are used to remove nitrate in water. These Iron nanoparticles are considered as cleaner productions that can be used for the efficient removal of nitrate [6]. In this method of green synthesis, there is no requirement for high pressure, energy, temperature or toxic chemicals. Hence nowadays many researchers are diverting themselves from using synthetic methods [7]. Zero-valent iron nanoparticles (nZVI) have already proven their efficacy in the reductive disposal of a wide array of environmental contaminants in numerous laboratory and field trials [8]. The synthesis of nZVI by the recently developed green bottom-up method is extremely promising [9].

Biosynthesis of metal nanoparticles extracted from different parts (mostly leaves) of the plant is the most effective process of synthesis at a very affordable cost. During the synthesis bioreduction of metal ions takes place. According to the researchers, the polyol components present in the plant extract are responsible for the reduction of iron ions whereas water soluble heterocyclic components stabilize the nanoparticles formed. Appropriate precursors such as ferric chloride can be used for the reduction of plant extracts [10-17].

Materials and Methods

Reagents and chemicals

Ferric Chloride ($FeCl_3$) and all analytical grade chemicals were purchased from TCI Chemicals, Chennai. Freshly prepared triple distilled water was used throughout the experiment.

Preparation of leaf extract by boiling method

Psidium guajava leaves were selected from Nagamalai area, Madurai, Tamilnadu, India on the basis of cost-effectiveness and ease of availability (**Figure 1**). Fresh and healthy leaves were collected locally and rinsed thoroughly first with tap water followed by distilled water to remove all the dust and unwanted visible particles, cut into small pieces.

About 10 g of these finely incised leaves were weighed and transferred into 250 mL beakers containing 100 mL distilled water and boiled for about 20 min. The extracts were then filtered thrice through Whatman No. 1 filter paper to remove particulate matter and to get clear solutions which were then refrigerated (4 °C) in 250 mL Erlenmeyer flasks for further experiments. In each and every step of the experiment, sterility conditions were maintained for the effectiveness and accuracy in results without contamination.

Figure 1 Image of Psidium guajava

UV-Vis spectra Analysis

Samples (1 mL) of the suspension were collected periodically to monitor the completion of bioreduction of Fe^{3+} in aqueous solution, followed by dilution of the samples with 2 ml of deionized water and subsequent scan in UV-visible (vis) spectra, between wavelengths of 200 to 700 nm in a spectrophotometer (Beckman - Model No. DU - 50, Fullerton), having a resolution of 1 nm.

FTIR analysis

FTIR analysis of the dried FeNPs was carried out through the potassium bromide (KBr) pellet (FTIR grade) method in 1:100 ratio and spectrum was recorded using Jasco FT/IR-6300 Fourier transform infrared spectrometer equipped with JASCO IRT-7000 Intron Infrared Microscope using transmittance mode operating at a resolution of 4 cm^{-1}.

Cyclic Voltammetry

Cyclic Voltammetry performed was in an analytical system model CHI-1205A and CHI-1205B potentiostat. A conventional three-electrode cell assembly consisting of an Ag/AgCl reference electrode, a Pt wire counter electrode and Glassy carbon Electrode (GCE) working electrode were used for the electrochemical measurements.

X-ray Diffraction (XRD)

The crystal structure of the produced FeNPs was determined and confirmed by using X-ray diffractometer (Model PW 1710 control unit Philips Anode material Cu, 40 KV,30 M.A, optics: Automatic divergence slit) with Cu Kα radiation λ=1.540 5 °A over a wide range of Bragg angles ($30° \leq 2\theta \leq 80°$). An elemental analysis of the sample was examined by energy dispersive analyses of X-rays with JED-2300 instrument. The crystallite domain size was calculated from the width of the XRD peaks, assuring that they are free from non-uniform strains. The particle size of the prepared sample was determined by using Scherrer′s equation as follows $D \approx 0.94\lambda/\beta\cos\Theta$, where D is the average crystallite domain size perpendicular to the reflecting planes, λ is the X-ray wavelength, β is the full width at half maximum (FWHM) and Θ is the diffraction angle.

Scanning Electron Microscopy – Energy Dispersive X-ray Spectrometry (SEM–EDX) Analysis

The microstructure and composite homogeneity of the obtained samples were investigated using a SEM/EDX scanning microscope JEOL-JSM 64000 LV. Energy dispersive X-ray analysis measurements were performed under standard conditions. The Iron nanoparticles were centrifuged at 10,000 rpm for 30 min and the pellet was redispersed in 10 mL ethanol and washed 3 times with sterile distilled water to obtain the pellet. The pellet was dried in an oven and thin films of dried samples (10 mg/mL) were used for compositional analysis.

Antibacterial activity by disc diffusion method

The anti-bacterial activity was done on human pathogenic *Bacillus cereus, Escherichia coli, Klebsiella pneumonia, and Staphylococcus aureus* by the standard disc diffusion method. The discs were soaked with double distilled water, plant leaf extract, Ferric chloride solution and a solution containing Iron nanoparticles of each type separately. Then the discs were air-dried in a sterile condition. Nutrient agar (NA) plates were seeded with 8h broth culture of different bacteria. Using sterilized dropping pipettes, different concentrations (10, 20, 30, 40 µl/well) of the samples were carefully added to the wells and allowed to diffuse at room temperature for 2 h. The plates were then incubated at 37 °C for 18-24 h. Gentamicin (10 µg) was used as positive control. Then, the maximum zone of inhibition was observed and measured for analysis against each type of test microorganism

Results and Discussion

Synthesis of Iron nanoparticles

The fresh leaves of Psidium guajava broth solution were prepared by taking 100g of thoroughly washed and finely cut plants in a 500ml Erlenmeyer flask along with 200ml of sterilized double distilled water and then boiling the mixture for 15min before finally decanting it. The extract was filtered through Whatmann filter paper no 1 and stored at -4°C. The filtrate was treated with an aqueous 1mM $FeCl_3$ solution in an Erlenmeyer flask and the mixture was heated at 60°-70°C for 10-15 minutes. As a result, a black colored solution was formed; indicating the formation of Iron nanoparticles. The Iron nanoparticle solution thus obtained was purified by repeated centrifugation at 10,000 rpm for 10 min.

As a black color solution was further confirmed by UV-Visible spectrum analysis. It showed that aqueous Iron ions could be reduced by aqueous extract of plant parts to generate extremely stable Iron nanoparticles in water (**Figure 2**).

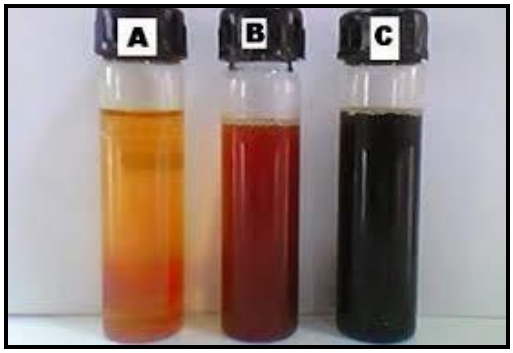

Figure 2 Formation of Iron nanoparticles and it is identification by the color change. (A) $FeCl_3$ solution, (B) plant extract (C) plant extract with $FeCl_3$ solution.

UV – Visible spectral analysis

Synthesized FeNPs using UV–visible spectroscopy were studied and the recorded spectra are shown in **Figure 3**. The absorption behavior shown in Figure 3 arises due to surface Plasmon resonance (SPR) [18]. As the Psidium guajava leaf extract was added to the aqueous $FeCl_3$ solution, the color of the solution changed from yellow to the black color indicating FeNPs formation. Figure 3 shows the UV-Vis spectra of the synthesized FeNPs which gives a broad absorption band at around 254.12nm. Such observation is characteristic of transition metal elements where the observed broad peaks are due to transitions within the filled and unfilled d-orbital compounded by influence from other external factors [19]. This peak at 254.12 nm has been shown to be due to the presence of the Iron nanoparticles in the Fe^0 state.

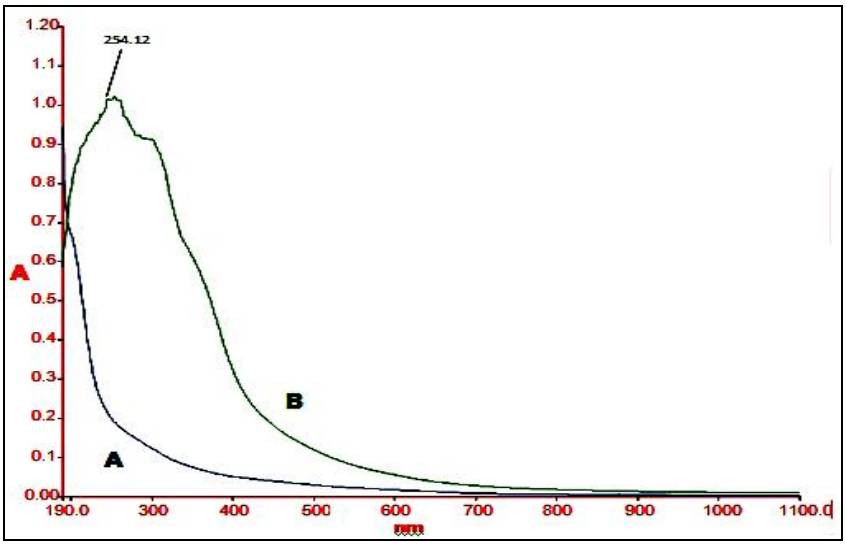

Figure 3 (A) UV-Visible absorption spectra of Psidium guajava leave extract. (B) UV-visible absorption spectra of synthesized Iron nanoparticles, showing thesurface plasmon resonance peak at 254.12 nm

FTIR analysis

FTIR analysis was carried out to identify the possible interaction between the biomolecules and Fe^{3+} during the biogeneric reduction reactions. The FTIR data for FeNPs containing Psidium guajava leaf extract is shown in **Figure 4**. The band at 3466 cm^{-1} is assigned for O-H stretching vibration of alcohol and phenol compounds and bands observed at 2075 cm^{-1}, 1637 cm^{-1}, 670 cm^{-1} are due to the C-O stretching, C=O stretching mode of the carbonyl functional groups in alcohol, ethers, acids, and esters. The carbonyl band at 1637 cm^{-1} was shifted to 1690 cm^{-1} during the formation of FeNPs. The shift in bands at 1690 cm^{-1} was clearly indicating the coordination of carboxylic acid with FeNPs and 688 cm^{-1} is attributed to zero valent iron, Fe^0 as reported in the literature.

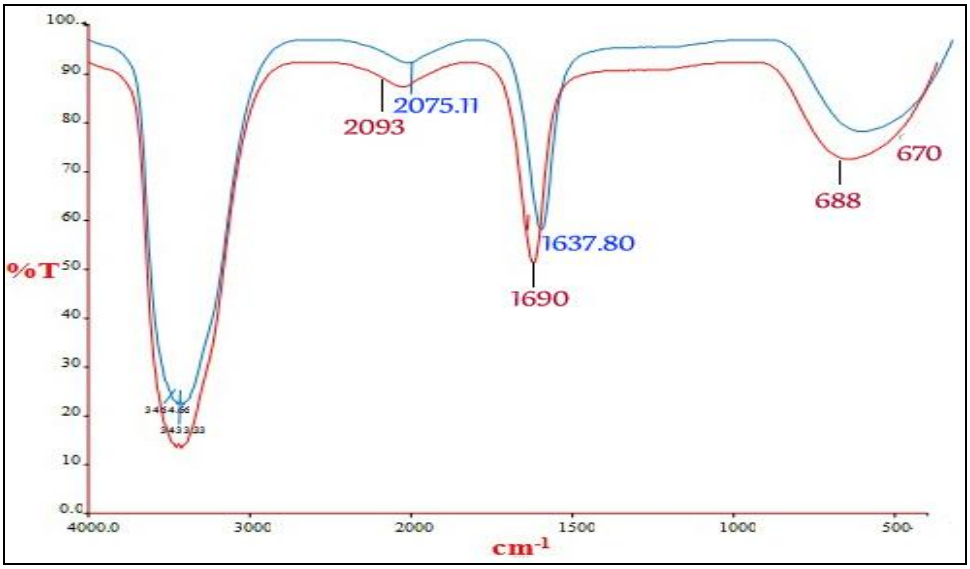

Figure 4 FTIR spectra of a) Psidium guajava leaf extract and b) Iron nanoparticles synthesized using the leaf extract of Psidium guajava

From the analysis of FTIR study, we revealed that the carbonyl group from the amino acid residue, carbohydrates, and phytochemical constituents has the stronger ability to bind metal NPs(capping of FeNPs) to prevent the agglomeration and thereby stabilize the medium. This suggests that biological molecules could possibly perform the dual function of formation and stabilization of FeNPs in the aqueous medium. Water soluble heterocyclic compounds such as flavonoids, alkaloids were mainly responsible for the reduction and stabilization of NPs. This results implied that tannins, spanin, flavonoids, steroids, carbohydrates, polyphenol, glycosides present in Psidium guajava leaf extract play a major role in the reduction of Fe^{3+} [20].

Cyclic voltammetry analysis

In the cyclic voltammetric analysis the addition of plant extract in the reaction medium, the anodic peak shifted towards the negative potential direction, implying that the reduced FeNPs are stabilized by plant extract. The extent of anodic peak current is greater than that of the cathodic peak current due to the fact that, a rate of reduction in iron ion may greater than oxidation. The cathodic peak represents the conversion of Fe^{3+}-Fe^{0}. The cyclic voltammogram of FeNPs shows the peaks observed at -0.458 volt and -0.100 volt.

The cyclic voltammogram of FeNPs has been shown in **Figure 5**. This might be because of the electron donating methoxy, hydroxyl and amine groups containing plant extract can provide a suitable environment for the formation of nanoparticles [21].

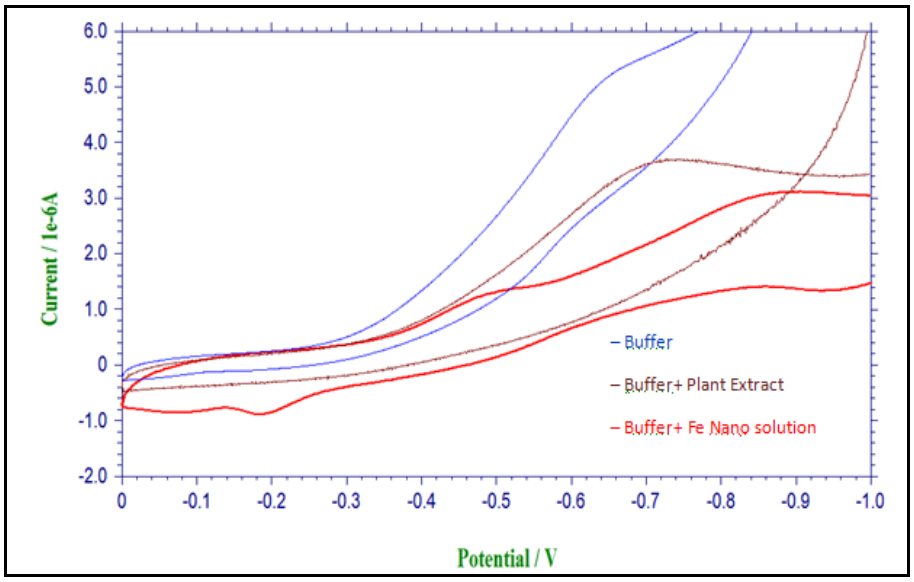

Figure 5 The cyclic voltammogram of a) Buffer solution b) Psidium guajava leaf extract and c) Iron nanoparticles synthesized using the leaf extract of Psidium guajava

X-ray Diffraction (XRD)

The sample of FeNPs could be also characterized by X-ray diffraction analysis of dry powders. The diffraction intensities were recorded from 10° to 80° at 2 theta angles (**Figure 6**). The results for FeNPs revealed four diffraction peaks [42(100), 44(002), 48(101), 77(110)] are indexed as cubic (JCPDS file no-655099). The mean size of nanoparticles is calculated using Debye-Scherrer's equation by determining the width of the (101) peak [22].

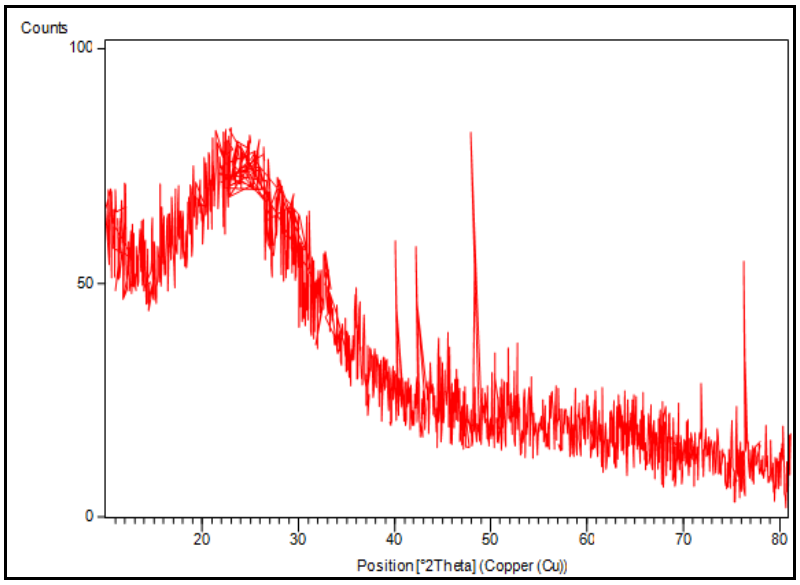

Figure 6 X-ray diffractograme of Iron nanoparticles

All the peaks in XRD pattern can be readily indexed to a hexagonal structure of Iron as per available literature. The size of the sample was calculated from the Scherrer's formula

$$= \frac{0.9 \times 1.54060 \times 10^{-10}}{5.1365 \times 10^{-3} \times 0.9999} = \frac{1.3867 \times 10^{-10}}{5.1359 \times 10^{-3}} = 27 \times 10^{-9} \text{ nm}$$

The size of Iron nanoparticles synthesized by green synthesis was estimated to be 27×10^{-9} nm

Scanning Electron Microscopy- Energy Dispersive X-ray Spectrometry (SEM-EDX) Analysis

The presence of elemental Iron can be seen in the graph presented by EDX, Which indicates the reduction of Iron ions to elemental Iron. The result of EDAX gives a clear idea about the elements present in the biosynthesized nanoparticles. The EDAX profile of phyto-capped FeNPs shows the strong signal of the Fe atom indicates the crystalline property as shown in **Figure 7** the vertical axis displays the number of X-ray counts whilst the horizontal axis displays energy in Kev. The optical absorption peak is at 7Kev which is typical for the absorption of metallic Iron nanocrystallites. Other than these signals for C, O are observed which may originate from the biomolecules capped to the surface of the FeNPs, Mn, and Cl due to plant constituents.

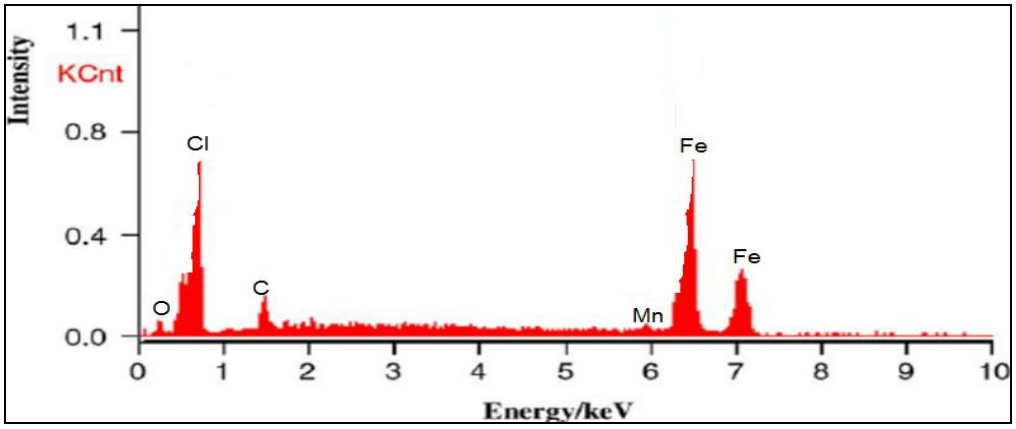

Figure 7 SEM-EDX profile of the synthesized Iron nanoparticles

To determine the morphology of the synthesized FeNPs the sample was analyzed with Scanning electron microscope (SEM). FeNPs synthesized using the extract of leaves of Psidium guajava are studied under SEM and shown in **Figure 8**. It indicates that FeNPs formed are agglomerated because of the adhesive nature having morphology of irregular appearance.

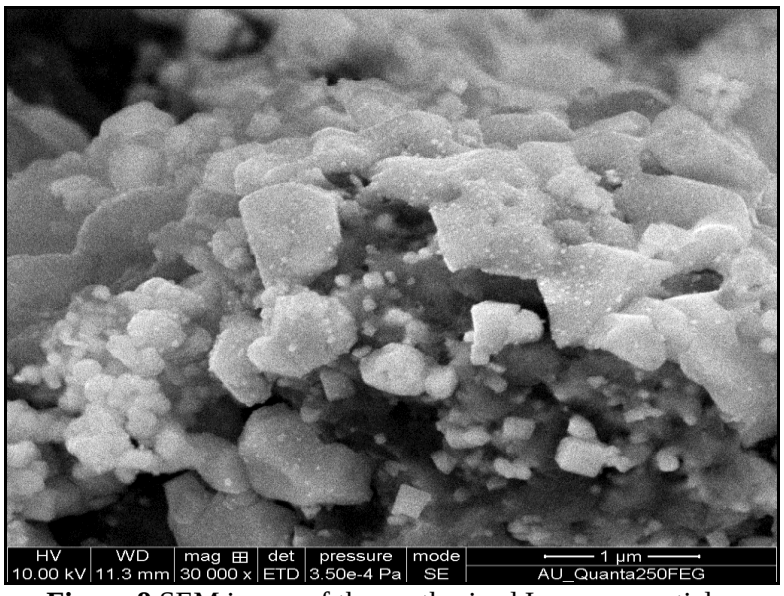

Figure 8 SEM image of the synthesized Iron nanoparticles

Antibacterial activity for FeNPs synthesized from Psidium guajava leaf extract

To investigate the antibacterial activity, four different bacteria were selected, of which two were Gram-positive and two were Gram-negative. The antibacterial activity was done on human pathogenic Gram-positive Bacillus cereus, Staphylococcus aureus, Gram-negative Escherichia coli, Klebsiella pneumonia by the standard disc diffusion method [23]. The FeNPs solution exhibits good antibacterial activity against the Gram-negative and Gram positive bacteria. The results are shown in **Table 1**. The cultures showed the radial diameter of the inhibiting zones of Bacillus cereus, Staphylococcus aureus, Gram-negative Escherichia coli, Klebsiella pneumonia is 14, 14, 17, 10 mm respectively. **Figure 9** represents the clear inhibition zone made by the FeNPs solution. The clear zone indicates bacterial growth restriction by the diffused FeNPs solution. The synthesized FeNPs have great potential due to their antibacterial activity. Thus the green synthesized nanoparticles have more effective antibacterial activity against the pathogens [24].

Table1 Effect of Iron nanoparticles on human pathogens

Pathogens	**Zone of Inhibition**	
	Plant Gold	**Gentamicin**
Bacillus cereus	14mm	22mm
Escherchia coli	17mm	21mm
Klebisella pneumonia	10mm	23mm
Staphylococcus aureus	14mm	25mm

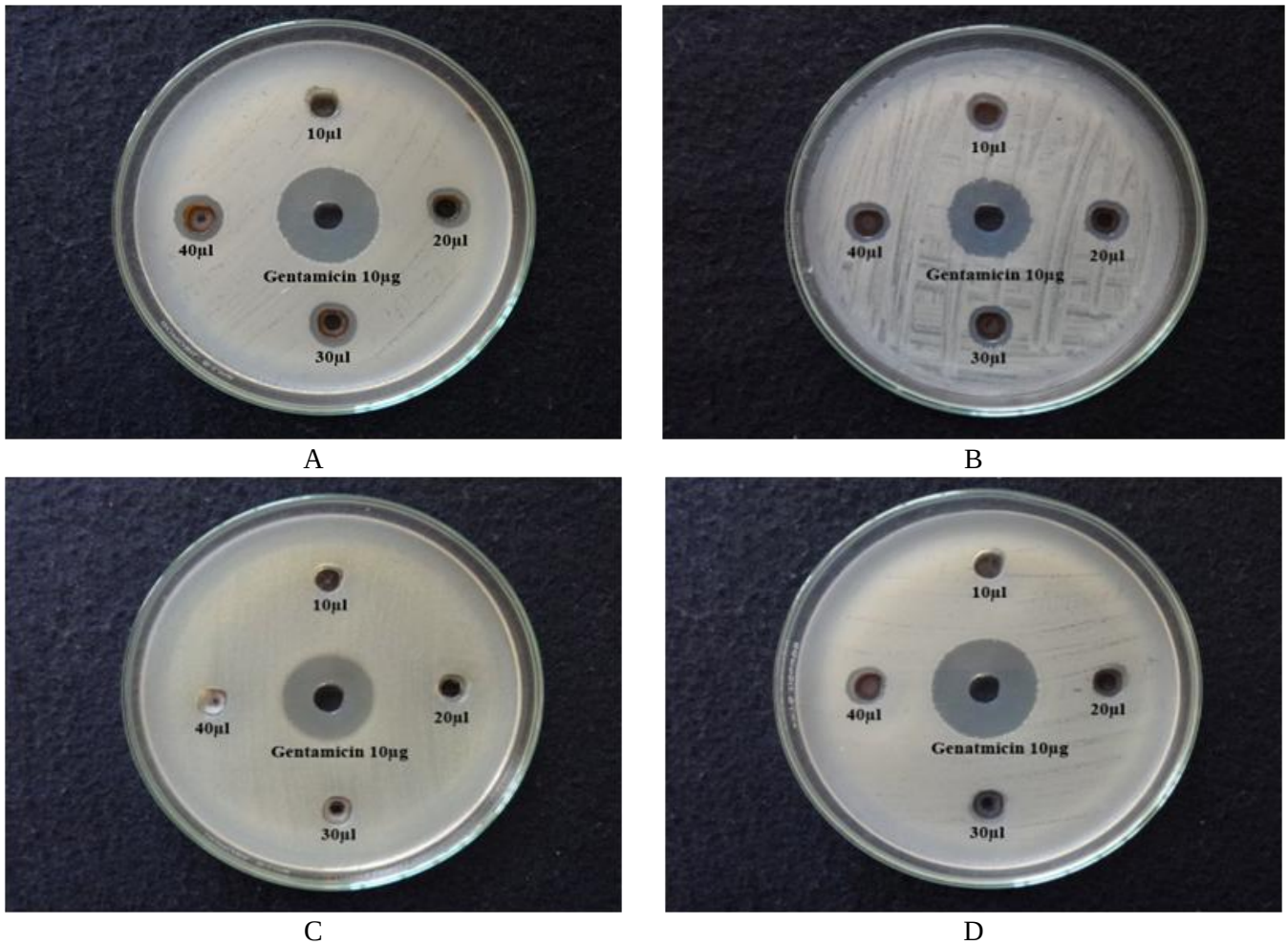

Figure 9 Antibacterial activity of Iron nanoparticles synthesized using the leaf extract of Psidium guajava against. (A) Human pathogenic *Bacillus cereus*. (B) *Escherchia coli*. (C) *Klebisella pneumonia*. (D) *Staphylococcus aureus* by the standard disc diffusion method

Conclusion

The extract of Psidium guajava plant may be capable of producing Iron nanoparticles. Under the UV-Visible wavelength, nanoparticles showed a surface Plasmon resonance behavior. The color change was also remarkable when Ferric Chloride was mixed with the reducing agent of plant extract. The biosynthesized FeNPs were characterized by UV-Vis spectroscopy, FTIR spectroscopy, XRD, Cyclic Voltammetry, SEM-EDAX and the antibacterial activity. From the XRD analysis, the average crystal of Iron nanoparticle was found to be 27nm. Overall, this approach is highly promising for the green sustainable production of FeNPs.

References

[1] Pattanayak, Monalisa, P. L. Nayak, International Journal of Plant, Animal and Environmental Sciences, 2013, 3(1), 68-78.
[2] M. Herlekar, S. Barve, R. Kumar, Journal of Nanoparticles, 2014, 2014, 1-9.
[3] T. Shahwana, S. Abu Sirriaha, M. Nairat, E. Boyacı, A.E. Eroglu, T.B. Scott, K.R Hallam, Chemical Engineering Journal, 2011, 172, 258–266.
[4] S. Machado, S.L. Pinto, J. P. Grosso, H. P. A. Nouws, J. T. Albergaria, C. Delerue-Matos, Science of the total environment, 2013, 445 - 446, 1-8.
[5] Monalisa Pattanayak, P. L. Nayak, World Journal of Nano Science & Technology, 2013, 2(1), 06-09.
[6] T. Wang, J. Lin, Z. Chen, M. Megharaj, R. Naidu, Journal of Cleaner Production. 2014, 83, 413-419.
[7] Y. Liu, S.A. Majetich, R. D. Tilton, D. S. Sholl, G. V. Lowry, Environmental Science & Technology. 2005, 39 (5), 1338–1345.
[8] Gabor Kozma, Andrea Ronavari, Zoltan Konya, Akos Kukovecz, ACS Sustainable Chemistry & Engineering. 2016, 4 (1), 291–297.
[9] S. Machado, JG. Pacheco, HP. Nouws, JT. Albergaria, C. Delerue-Matos, Science of the total environment. 2015, 15(533), 76-81.
[10] W. C. W .Chan, D. J. Maxwell, X. Gao, R. E. Bailey, M. Han, S. Nie, Current Opinion in Biotechnology, 2002, 13(1), 40-46.
[11] A. Thess, R. Lee, P. Nikolaev, H. Dai, P. Petit, J. Robert, C. Xu, Y. H. Lee, S. G. Kim, A. G. Rinzler, Science, 1996, 273(5274), 483-487.
[12] B. Z. Zhan, M. A. White, T. K. Sham, J. A. Pincock, R. J. Doucet, K. V. R. Rao, K. N. Robertson, T.S. Cameron, Journal of the American Chemical Society, 2003, 125(8), 2195-2199.
[13] A. L. Linsebigler, G. Lu, J. T. Yates, Chemical reviews. 1995, 95 (3), 735–758.
[14] H. Zhang, R. L. Penn, R. J. Hamers, J. F. Banfield, J. Phys. Chem., B., 1999, 103 (22), 4656–4662.
[15] R. F. Service, Science, 1998, 281(5379), 940-942.
[16] N. L. Rosi, D. A. Giljohann, C.S. Thaxton, A. K. R. Lytton-Jean, M. S. Han, C.A. Mirkin, Science, 2006, 312(5776), 1027-1030.
[17] D. G. Shchukin, J. H. Schattka, M. Antonietti, R. A. Caruso, J. Phys. Chem. B., 2003, 107(4), 952-957.
[18] R. Veerasamy, TZ. Xin, S. Gunasagaran, TFW. Xiang, EFC. Yang, N. Jeyakumar, Journal of Saudi Chemical Society, 2011, 15(2), 113-120.
[19] I. N. Michiraa, D.N. Katithib, P. Gutoc, G. N. Kamaud, P. Bakere, E. Iwuohaf, International Journal of Sciences: Basic and Applied Research, 2014, 13(2), 63-76.
[20] R. Kiruba, G. Alagumuthu, International journal of Pharmacy, 2014, 4(4), 195-200.
[21] E. Laviron, Journal of Electroanalytical Chemistry and Interfacial Electrochemistry 1979, 101(1), 19-28.
[22] K. Shameli, MB. Ahmad, M. Zargar, WM. Yunus, A. Rustaiyan, NA. Ibrahim, International Journal of Nanomedicine, 2011, 2011(6), 581-590.
[23] Renu Geetha Bai, Kasturi Muthoosamy, Fiona Natalia Shipton, Alagarsamy Pandikumar, Perumal Rameshkumar, Nay Ming Huang, Sivakumar Manickam, RSC Advances, 2016, 6, 36576–36587.
[24] P. Shanmuga Praba, J. Jeyasundari, Y. Brightson Arul Jacob, Eur. Chem. Bull., 2014, 3(10), 1014-1016.

Publication History
Received 06th May 2017
Revised 27th May 2017
Accepted 12th June 2017
Online 30th June 2017